NeuroImage xxx (2008) xxx–xxx

Contents lists available at ScienceDirect

NeuroImage

journal homepage: www.elsevier.com/locate/ynimg

Functional reorganization in rat somatosensory cortex assessed by fMRI: Elastic image registration based on structural landmarks in fMRI images and application to spinal cord injured rats

Esther Sydekum [a], Christof Baltes [a,1], Arko Ghosh [b,1], Thomas Mueggler [a], Martin Schwab [b], Markus Rudin [a,c,*]

[a] Institute for Biomedical Engineering, University and ETH Zurich, Switzerland
[b] Brain Research Institute, University of Zurich, Switzerland
[c] Institute of Pharmacology and Toxicology, University of Zurich, Switzerland

ARTICLE INFO

Article history:
Received 20 July 2008
Revised 19 September 2008
Accepted 10 October 2008
Available online xxxx

ABSTRACT

The accuracy at which changes in cortical functional topology can be assessed by functional MRI (fMRI) depends on the quality of the reference coordinate system used for comparison of data sets obtained in different imaging sessions. Current procedures comprise an overlay of activation clusters on registered high-resolution anatomical images. Yet, fMRI images are frequently distorted due to susceptibility artifacts, which are prominent in rodent studies due to the small dimensions involved and high magnetic field strengths used. Therefore, a procedure for co-registration of activation maps has been developed based on anatomical landmarks defined on fMR echo planar images (EPI) themselves. Validation studies in control rats revealed that the centers of activated areas in somatosensory cortex S1, evoked through sensory forepaw stimulation fell within an area of 1×1 mm^2 in agreement with known electrophysiological coordinates. The technique was applied to detect changes in activation patterns in rats following smaller unilateral spinal cord injuries (SCI) in their cervical segments (C3/C4) 12 weeks after lesion. Despite of an almost complete behavioral recovery, fMRI responses remained altered in SCI animals with both significantly reduced fMRI signal amplitude and reduced latency to reach the peak response. Moreover, in SCI animals the activated S1 area corresponding to the contralesional forepaw was significantly enlarged and the center-of-mass for the ipsilesional paw was shifted rostrally. The mapping technique described combined with the temporal analysis of the BOLD response enabled a noninvasive quantitative characterization of cortical functional reorganization following SCI in rats.

Introduction

Experimental neuroscience has developed a variety of tools to map brain functional architecture and assess its changes in response to a challenge. The rodent brain is well suited for such studies due to its well characterized topological organization. For example, the rat somatosensory cortex (S1) has been investigated using highly accurate electrophysiological techniques (Chapin and Lin, 1984; Coq and Xerri, 1999; Xerri et al., 2005), even distinguishing contributions from different cortical layers (Neafsey, 1990). Similarly, optical methods such as intrinsic optical recordings provided information about the neurovascular coupling with high spatial and temporal resolution (Sheth et al., 2003; Sheth et al., 2004). Functional magnetic resonance imaging (fMRI) is non-invasive and allows to longitudinally follow changes in several brain areas in single animals over time, but when compared to the methods mentioned above, i.e. electrophysiological readouts, fMRI is limited by its relatively low spatial resolution of the order of typically 200–400 μm in rats (Sauter et al., 2002; Weber et al., 2006). Although spatial and temporal resolution are progressively improved, there is an ultimate resolution limit defined by the nature of the hemodynamic signal itself (Logothetis, 2008).

In fMRI studies a number of different sensory stimuli have been applied to map the somatosensory areas of S1 such as electrical stimulation of forepaw (Hyder et al., 1994; Marota et al., 1999; Van Camp et al., 2006), hindpaw (Bock et al., 1998), and tail (Spenger et al., 2000), or mechanical stimulation of whiskers (Yang et al., 1997; Kennerley et al., 2005). In these studies the functional response was detected via the so-called blood-oxygenation level dependent (BOLD) contrast, which depends on the integrity of the neurovascular coupling. Changes in the ratio of oxygenized versus deoxygenized hemoglobin alter the R_2* relaxation rate, and are commonly detected using R_2* sensitive gradient-echo sequences such as fast-low angle

* Corresponding author. AIC — ETH Zurich, HCI D426, Wolfgang-Pauli-Str. 10, CH-8093 Zürich, Switzerland. Fax: +41 44 633 11 87.
E-mail address: rudin@biomed.ee.ethz.ch (M. Rudin).
[1] CB and AG contributed equally to this work.

1053-8119/$ – see front matter © 2008 Elsevier Inc. All rights reserved.
doi:10.1016/j.neuroimage.2008.10.015

shot (FLASH (Frahm et al., 1986; Grune et al., 1999)) or echo planar imaging (EPI (Mansfield, 1984; Keilholz et al., 2004)).

In most rodent fMRI studies involving somatosensory stimulation a coronal slice orientation has been used (we use the nomenclature of the rat brain atlas by 'Paxinos and Watson (1998)'). This is suboptimal for assessing the topology of activated cortical areas as signals are averaged over the thickness of the imaging slice and for multislice acquisitions certain areas might be omitted due to potential gaps in-between adjacent slices. Coronal sections yield high resolution in the coronal plane (Stefanovic et al., 2007), but lower spatial resolution perpendicular to it, i.e. in a horizontal plane. The spatial accuracy required for detecting small topological changes within rat cortical structures following a pathological event might therefore not be sufficient. In view of the fact that rat cerebral cortex is devoid of gyration and organized as a quasi two-dimensional map representing the various body regions, a horizontal slice orientation is optimally adapted for monitoring changes in cortical functional topology in both caudal–rostral and lateral directions also enabling the characterization of forepaw and hindpaw in one imaging slice (Chen and Shen, 2006).

Proper registration of fMRI data sets is a critical step for the accurate mapping of changes in functional topology over time. The common procedure in animal studies is to register high resolution anatomical reference images, which are commonly acquired using spin echo pulse sequences that provide high contrast-to-noise ratio and good anatomical definition. These images are largely devoid of geometrical distortions due to magnetic susceptibility artifacts and rigid body transformations are, in general, sufficient to achieve a high degree of co-alignment. The respective transformation matrices are then used to process EPI-derived BOLD data and the transformed activation clusters are overlaid on the registered high-resolution images. However, in contrast to spin echo images, EPI images are highly sensitive to changes in magnetic susceptibility and therefore likely to be distorted with regard to the anatomical reference data (Jezzard and Clare, 1999). This effect becomes more prominent at high magnetic field strength as used in this study (Grieve et al., 2000; Zhao et al., 2005).

To avoid introducing additional errors, registration of fMRI data should be carried out with EPI images directly. This requires the identification of reproducible structural landmarks in EPI images. Suitable landmarks on coronal EPI images comprising the rat cerebral cortex have been identified: 1) the cerebral midline, 2) the anterior end of the cerebellum, 3) a highly reproducible signal void in EPI images, which is located directly below the sutura coronalis thereby allowing the identification of the Bregma coordinates, and 4) the maximum hemispheric width of the cerebrum. We have used these landmarks to elastically map EPI fMRI images of individual animals to a standard rat brain coordinate system (Paxinos et al., 1985). Before applying the registration procedure to study plasticity in CNS lesion models, careful validation using fMRI data from control animals and comparison with literature data was mandatory. This was achieved by using a sensory stimulation paradigm: electrical stimulation of both forepaws and one hindpaw, which evoked fMRI responses that were strictly confined to the contralateral cortical S1 area.

In order to assess the sensitivity of the mapping procedure in detecting changes in functional topology following a CNS insult rats subjected to spinal cord injury (SCI) have been studied. Young rats (post-natal day 28) were lesioned at the cervical segment (C3/C4) and fMRI experiments were performed at week 12 and later following a phase of adaptation and recovery. At this stage, most rats had reached almost full performance in the behavioral test applied assessing skilled walking. Nevertheless, the BOLD response was different as compared to age-matched control animals: alterations in both the topology and the temporal signature of the BOLD signal have been observed.

Method

Animals

Male Lewis rats ($n = 21$) of 250 g body weight have been used for the experiments. Animals had free access to standard rat chow and tap water. Four rats have been used for the characterization of the Bregma landmark, eight for evaluation of the accuracy of the registration procedure by analyzing the reproducibility of S1 activation during forepaw and hindpaw stimulation, four rats were included in the SCI study. Five additional rats have been used to assess changes in mean arterial blood pressure (ΔMABP) in response to the stimulation protocol applied. All animal experiments were performed in strict adherence to the Swiss Law for Animal Protection approved by the veterinary office of the canton of Zurich, Switzerland.

Spinal cord injury (SCI) model

Spinal cord lateral hemisection injuries were performed in young rats (P 28) deeply anaesthetized with a subcutaneous (s.c.) injection of Hypnorm (120 μl/200 g body weight; VetaPharma LtD, Leeds, England) and Dormicum (0.75 mg in 150 μl/200 g body weight; Roche Pharmaceuticals, Basel, Switzerland). By counting of vertebral spines from segment T-2 vertebral segment C-4 (corresponding to spinal segment C-3/4) was identified. A dorsal unilateral (left side) laminectomy was performed at C-4 to expose the dura covered spinal cord. The dura was removed using blunt iridectomy scissors and fine forceps. Subsequently the lateral spinal cord was cut using fine iridectomy scissors. Post surgery, animals were placed on a warm pad till awake. For the following 5 days pain reducing and antibiotic medication was injected. Bladders were emptied twice a day until bladder function was completely recovered.

Behavior test

As behavior test paradigm to quantify skilled locomotion after spinal cord injury the horizontal ladder (60 cm ladder with 6 cm gaps) has been used (Metz et al., 2000; McEwen and Springer, 2006). The animal's performance was tested at eight and ten weeks after injury (fMRI at week 12). When the forepaw was placed on the rung to support the animal's bodyweight, it was noted as a successful step.

For SCI animals the terms *ipsilesional* and *contralesional* paw have been used to indicate the paw in relation to the side of the spinal cord lesion. This should not be confounded with the response evoked in the cortical S1 region, which was in all cases strictly *contralateral* to the paw stimulated. For control animals we simply use the terms left and right paw.

Animal preparation for MR experiments

Rats were anaesthetized with an initial dose of 4% isoflurane in an air/oxygen (4:1) mixture using an induction chamber, endotracheally intubated with a tube made from polyethylene (PE; inner/outer diameter, 1.4/1.9 mm) and actively ventilated at a rate of 50 breaths per minute (BpM) using a small animal ventilator (Maraltec, Biel-Benken, Switzerland). A single dose of 15 mg/kg of the neuromuscular blocking agent gallamine (Sigma-Aldrich, Germany) was administered intravenously (i.v.) through the tail vein to facilitate ventilation and to avoid motion artifacts during fMRI data acquisition. The animals were positioned on a support made from Plexiglas. Anaesthesia level was maintained at 1.5% isoflurane throughout the experiment. Body temperature was recorded with an MRI compatible rectal probe and maintained at a physiological level using warm air. Furthermore carbon dioxide partial pressure, pCO_2, was monitored using a transcutaneous electrode attached to the rat abdomen (TCM4, Radiometer Copenhagen).

Please cite this article as: Sydekum, E. et al., Functional reorganization in rat somatosensory cortex assessed by fMRI: Elastic image registration based on structural landmarks in fMRI images and application to spinal cord injured rats, NeuroImage (2008), doi:10.1016/j.neuroimage.2008.10.015

In five additional control rats mean arterial blood pressure change (ΔMABP) was measured (PowerLab, AD Instruments Inc., Spechbach, Germany) in response to the 6 mA stimulation. The major tail artery was cannulated with a catheter and blood pressure changes were recorded in mmHg using a pressure transducer. Physiological conditions were controlled as in fMRI experiments.

MRI/fMRI experiments

MRI/fMRI experiments were performed on a Bruker Biospec 94/30 small animal MR system (Bruker BioSpin GmbH, Karlsruhe, Germany) operating at 400 MHz. The gradient coils are capable of generating a maximum strength of 400 mT/m with a minimum rise time of 80 μs. A radiofrequency (RF) cross-coil setup has been used with a linearly polarized birdcage resonator (inner diameter 67 mm, length of resonating structure 70 mm) for RF transmission and a quadrature surface coil (length 30 mm, width 26 mm) for signal reception.

Two horizontal slices serving as anatomical reference images for the fMRI data were acquired (Fig. 1a) using a multi-slice (RARE) spin echo sequence (Hennig et al., 1986) with the following acquisition parameters: field-of-view (FOV)=33×25 mm^2, matrix dimension (MD)=256×128, slice thickness (SLTH)=1 mm, inter-slice distance (ISD)=1.25 mm, repetition delay (TR)=1259 ms, echo delay (TE)=25 ms, effective echo delay (TE_{eff})=60 ms, RARE factor=8, number of averages (NA)=1, image acquisition time (T_{acq})=1.25 min. fMRI experiments based on the BOLD contrast were carried out by recording single shot gradient echo-EPI (GE-EPI) images (FOV)=33×25 mm^2, MD=64×64, SLTH=1 mm, ISD=1 mm, TE/TR=10 ms/1250 ms, NA=8, image acquisition time=10 s, number of repetitions (NR)=50. The slice position corresponded to the anatomical images. In order to minimize image distortions and susceptibility artifacts the homogeneity of the magnetic field was improved by optimizing magnetic field corrections corresponding to first and second order spherical harmonics (first and second order shims) using the FASTMAP algorithm (Gruetter, 1993).

fMRI: Sensory stimulation paradigm

For sequential electrical stimulation two bipolar platinum needle electrodes (Genuine Grass instruments, West Warwick, USA) were subcutaneously placed on each forepaw. The leads were outside the RF field of both transmit and receiver coil and therefore did not cause any image artifacts. Moreover, they were filtered to avoid pickup of unwanted RF signals. A PowerLab (AD Instruments Inc., Spechbach, Germany) stimulator supplied rectangular pulses with current amplitude, pulse duration and frequency set to 6 mA, 0.5 ms, and 3 Hz, respectively. A block design stimulation paradigm has been used with a 60 s off and 40 s on cycle. This basic module was repeated 5 times, leading to an overall duration of the fMRI data acquisition of 500 s for one paw.

Characterization of the Bregma landmark using MRI angiography

In order to demonstrate the vascular origin of the hypo-intense structure underneath the coronal suture, MR angiographic studies have been carried out in four rats. In addition to the MR experiments described above, an additional RARE data acquisition was carried out with identical parameters except the SLTH, which was reduced to 0.5 mm. In the high-resolution anatomical RARE images in-plane vessels appear as dark structures due to spin dephasing of protons in

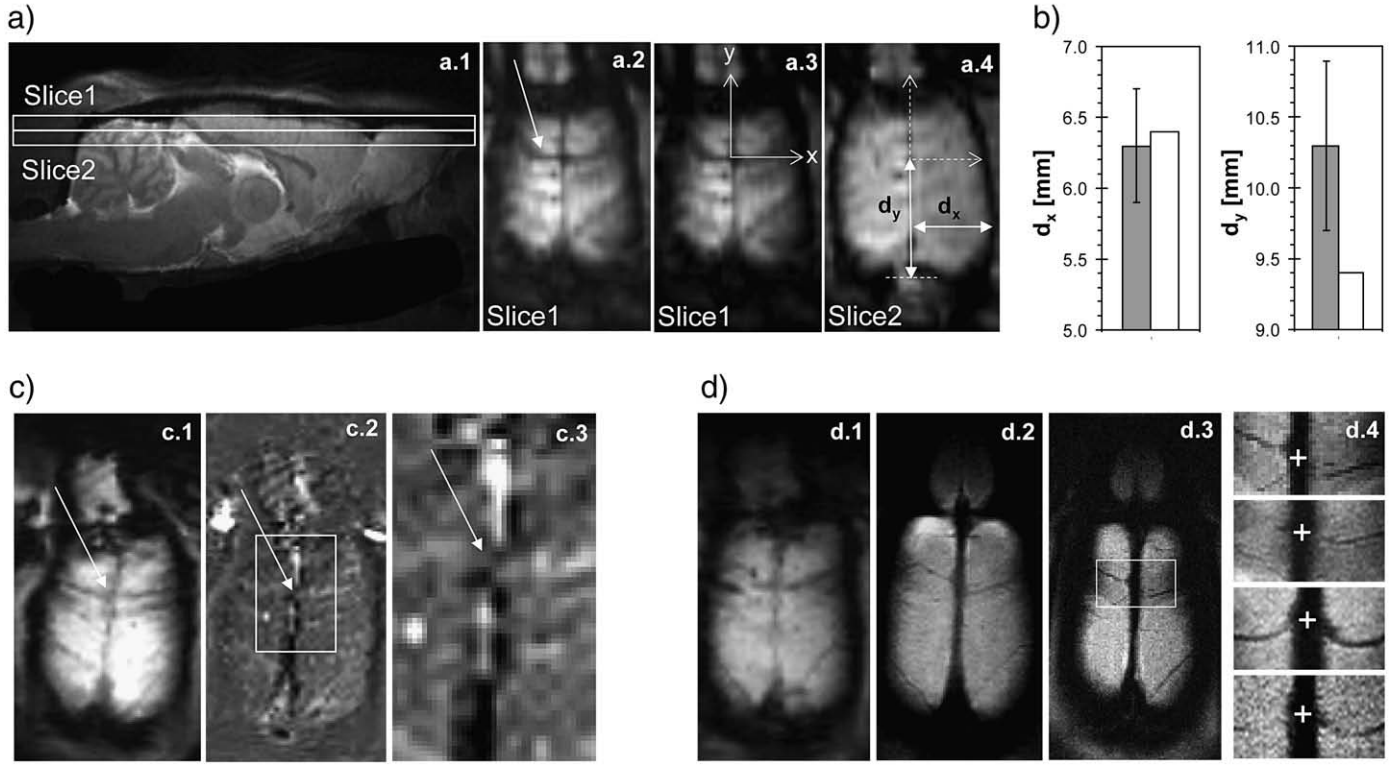

Fig. 1. (a) Mid-sagittal cross-section through rat brain with the 2 horizontal sections used for fMRI experiments indicated (left). The echo planar image (EPI) of horizontal slice 1 (Slice1) shows the artifact due to the vessel underneath the coronal suture (arrow). The intersection of the artifact with the cerebral midline defines the Bregma point (a2), which is taken as the origin for the coordinate system (a3). The scaling factor for the bilinear elastic registration is defined from the distance d_y between the Bregma and the rostral end of the cerebellum and the maximum width d_x of the hemisphere (a4). (b) Comparison of values d_x and d_y taken from EPI images and from rat brain reference atlas (open bar). (c) Contrast enhanced angiography for identification of vessels. Reference image (c1) shows artifact prior to administration of contrast agent (Sinerem®). The middle panel displays difference image prior – post contrast agent administration, showing hyper-intensity of vascular structure (c2) with a blow-up of the central region (c3). (d) Comparison of EPI (d.1) with high resolution spin echo images of the same slice recorded with a thickness of 1 mm (d.2) and 0.5 mm (d.3), respectively. The vessels causing the artifact are clearly visible. The variability of the vasculature in four rats is shown in the panels (d.4) with the Bregma point as derived from the rat brain reference atlas indicated (white cross).

Please cite this article as: Sydekum, E. et al., Functional reorganization in rat somatosensory cortex assessed by fMRI: Elastic image registration based on structural landmarks in fMRI images and application to spinal cord injured rats, NeuroImage (2008), doi:10.1016/j.neuroimage.2008.10.015

flowing blood. These images were complemented by a contrast-enhanced MR angiogram. For this, Sinerem® (Laboratoire Guerbet SA, Roissy, France), a contrast agent based on iron-oxide nanoparticles with a plasma half-life of 5.5 h (Benderbous et al., 1996), was administered via the tail vein at an iron dose of 10 mg/kg. MR images were recorded using the GE-EPI sequence as described above. Difference images prior minus post contrast agent administration revealed major cortical vessels (veins).

Data analysis

a) fMRI analysis

Data analysis of the fMRI time series for individual animals was performed using Biomap software (4th version, M. Rausch, Novartis Institute for Biomedical Research, Basel, Switzerland). For statistical analysis of the effects of peripheral stimulation on brain activity, parametric maps were calculated using the general linear model (GLM). Statistical maps were computed with regard to a boxcar reference using as threshold for the p value $p \leq 0.01$. As a second criterion activation clusters had to be larger than 5 voxels. For regions-of-interest (ROIs) fulfilling both criteria the area (number of voxels exceeding the p-threshold) and the averaged amplitude within the appropriate somatosensory area was calculated for each data set. The average change in the BOLD signal intensity in percent of the baseline values ($\Delta S_{BOLD}(\%)$) was obtained by calculating for each rat the average of the difference in signal intensities during the 5 stimulation periods ($S_{on}(i)$ for $i=1$ to 5) minus the average baseline amplitude divided by the average baseline amplitude (amplitude during resting period prior to the first stimulation phase, $S_{off}(1)$).

No additional processing steps such as filtering have been applied when computing the $\Delta S_{BOLD}(\%)$ versus time curve. No detrending of the raw data has been used, as slow signal drifts might contain relevant information about different signal components. For display purposes, images have been smoothened by bilinear interpolation. Yet, all quantitative analyses have been carried out using non interpolated raw data. In general, data post processing was kept at a minimum to minimize potential signal distortions and to illustrate the quality of the fMRI raw data.

b) Mapping onto the reference coordinate system

To facilitate comparison within and between groups normalization to the coordinate system of the Paxinos rat brain atlas (Paxinos and Watson, 1998) was performed. From the two horizontal cross-sections recorded the fMRI coordinate system was defined as follows (Figs. 1a, b): the origin of the right-hand coordinate system was chosen at the intersection of the horizontal suture line with the brain midline (sagittal suture), corresponding to the projection of the Bregma point onto the upper imaging plane. The directions of the coordinate axes were defined along the midline direction (y-axis) and perpendicular to it (x-axis). For axis scaling the distance between the Bregma projection and the anterior end of the cerebellum at the brain midline (d_y), and the maximal width of the right hemisphere in the lower section (d_x) were selected as a scale reference (Fig. 1b). Using the lower section for d_x determination reduced uncertainties due to smaller partial volume effects caused by the curvature of the brain surface. Comparing the distances d_x, d_y with the respective distances in the Paxinos rat brain atlas (Paxinos and Watson, 1998) yielded the scaling factors s_x, s_y used for linear scaling of the EPI images. The spatial normalization procedure was carried out using an IDL-based software developed in-house.

In order to compare the spatial loci of the activation in cortical S1, centers-of-mass (CMA) for the activated areas were calculated using t-values as the weighting function (1st moment, as t-values are based on a linear scale; (Duong et al., 2000)). As a second parameter the center of the activation area (CEN) was determined based on geometrical considerations only (0th moment). More over, for each individual animal the absolute value of the difference of CMA and CEN (abs(CMA–CEN)) was calculated, accounting for asymmetry in the t-value distribution.

Post-mortem reconstruction of the injury site

Within one week after BOLD-fMRI, animals were overdosed with Nembutal and perfused with 400 ml ringer solution containing 4% PFA and 5% sucrose. Spinal cords were immediately removed and postfixed overnight in the same solution. The tissue was immersed in 30% sucrose prior to being frozen and cross-sectioned (50 μm thick at 100 μm gaps) and collected on a glass coverslip. These sections were reconstructed using Neurolucida (final magnification, 200×; Neurolucida 7.0; MicroBrightfield, USA), delineating the damaged tissue.

Results

Definition of reference coordinate system

The position of the two horizontal image planes used for the fMRI experiments and the definition of the corresponding reference coordinate system are displayed in Fig. 1a. Characteristic landmarks have been identified on the GE-EPI images defining the reference points for the coordinate system: 1) the 'Bregma' (origin of the coordinate system) defined by the intersection of the hypo-intense line following the coronal fissure (sutura coronalis) and the cerebral midline in the section S1, 2) the rostral end of the cerebellum in section S2 (Xiao, 2007), and 3) the maximum width of the cerebrum also in section S2. MR angiography experiments were carried out to test the hypothesis that vessels underlying the fissure might be the cause of the signal void and to assess the accuracy of this so-called Bregma point. For this purpose two approaches have been pursuit: a first based on contrast enhanced MRA using Sinerem®, an intravascular contrast agent, and the second based on high-resolution coronal spin-echo imaging, as in-plane vessels appear hypo-intense when using this sequence due to spin dephasing. Following Sinerem® injection a significant signal decrease was observed in cerebral vessels including the vessel underlying the suture, thereby indicating that the signal void is in fact due to a vascular contribution (Fig. 1c). An iron-oxide dose of 10 mg/kg proved to be optimal for our purpose as higher concentrations enhanced the vessel in the difference image, but also led to a loss of spatial accuracy due to susceptibility effects such as widening of structures (blooming effect), and shift in position due to a shift in resonance frequency. For the proposed registration procedure a match of the coordinates of the suture lines (hypo-intense structure in the EPI images) and the underlying vessels, as derived from the MRA experiment, is crucial, as they define the origin of the reference system. These findings were corroborated by high spatial resolution spin echo images acquired with strong T_2 weighting, which clearly identify the vessels at the respective position. The variability in vascular topology at the 'Bregma' site (the Bregma position derived from the reference atlas is indicated by a white cross in Fig. 1d) is minimal as shown by the spin echo MRA of four different rats displayed in Fig. 1d. The vascular origin of the hypo-intense EPI structure was confirmed surgically: removal of the skull revealed the underlying vessels.

The reference distances, Bregma to rostral end of cerebellum (d_y) and maximal width of the cerebrum (d_x) from EPI images were compared with the respective values from the Paxinos atlas of rat brain (Fig. 1b). While a deviation of 0.9±0.6 mm was found for d_y, which was significantly longer for EPI images as compared to the reference atlas (10.3±0.6 mm versus 9.4 mm), the deviation for d_x was found minimal (6.3±0.4 mm versus 6.4 mm). Correspondingly, EPI images were mapped individually on the brain atlas using linear elastic scaling with scaling factors in the range of 0.88 to 0.96 for the y- and 0.97 to 1.01 for the x-direction. To test whether these

Please cite this article as: Sydekum, E. et al., Functional reorganization in rat somatosensory cortex assessed by fMRI: Elastic image registration based on structural landmarks in fMRI images and application to spinal cord injured rats, NeuroImage (2008), doi:10.1016/j.neuroimage.2008.10.015

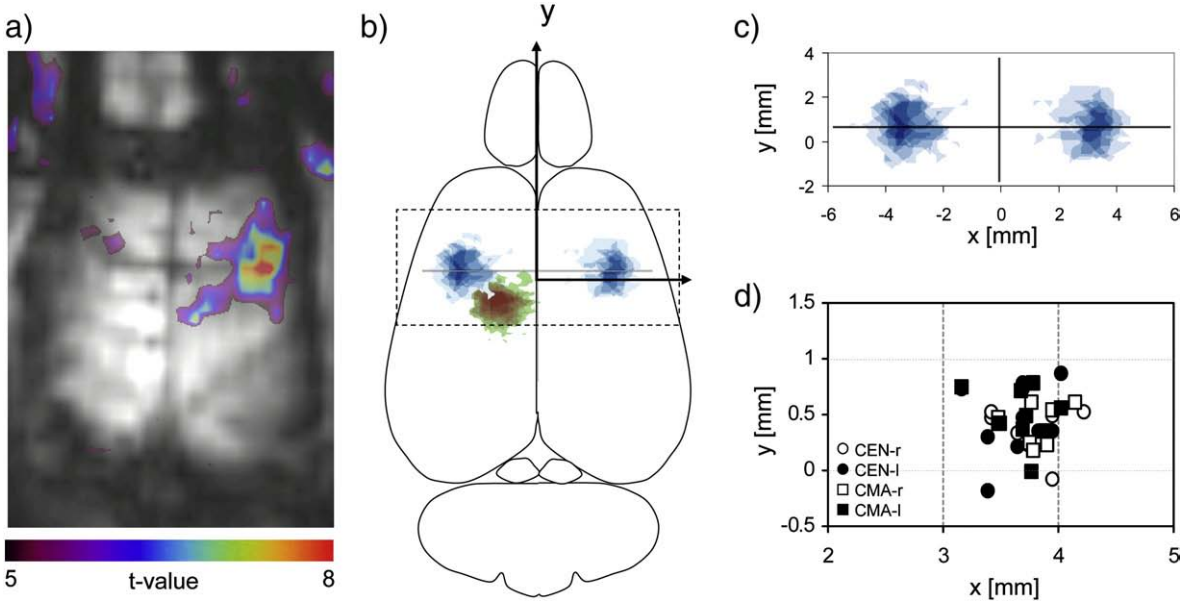

Fig. 2. BOLD fMRI during electrical fore and hindpaw stimulation in healthy Lewis rats: (a) overlay of activity map on EPI images for a representative animal for stimulation of left forepaw. A unilateral response confined to the somatosensory area S1 is observed. (b) Group analysis for eight healthy Lewis rats for stimulation of both fore (blue) and right hindpaw (brown). Data have been co-registered as described in the text. The activated areas are displayed in semi-transparent manner, the intensity of the color indicating the number of animals. Note high degree of reproducibility of BOLD response among the eight animals and clear segregation of fore and hindpaw area with minimal overlap. (c) High resolution activation maps for forepaw stimulation in relation to the coordinate system. (d) Quantitative analysis of fMRI response. Shown are the centroid (CEN) and center-of-mass (CMA) of the activated brain areas for the individual rats for stimulation of the right (r) and left (l) forepaw. Data for the right forepaw have been mirrored to demonstrate the high degree of symmetry in the fMRI response.

differences between individual EPI scans have methodological reasons or are due to true biological variations, brain dimensions of rats were measured on anatomical images based on a spin-echo pulse sequence (n=4). The brain size showed no detectable variations: within error limits there was no variation among the animals studied regarding the cerebral width d_x (6.4±0.0 mm, mean±SE) and only minor variability for d_y (9.4±0.1 mm). Both values are in excellent agreement with the values derived from the reference rat brain atlas (d_x=6.4 mm, d_y=9.4 mm).

Validation of registration procedure: generation of functional brain maps

Sensory stimulation of fore and hindpaws led to BOLD signal changes in the contralateral somatosensory cortices as illustrated by the t-score functional map, which is overlaid on the corresponding coronal echo-planar image of the rat brain for the stimulation of the left forepaw of a representative animal (Fig. 2a) (6 mA, 3 Hz, 0.5 ms, 40 s on, 60 s off, 5 cycles). In Fig. 2b activation maps for left and right forepaw and right hindpaw stimulation are superimposed and displayed with regard to the reference coordinates. For orientation the outer contour of the brain is indicated. The activated regions of individual animals are displayed at a uniform intensity level for all voxels that exceed the threshold p-value in both sections; hence, the intensity of the color reflects the number of animals showing an fMRI response at the respective location. The shapes of the activated cortical regions for all animals tested were highly similar and displayed a high degree of overlap. Hind and forepaw areas were found adjacent with no overlap. Overlaying the activation maps of individual animals (Fig. 2b) would allow an immediate identification of outliers, which might bias results of a group analysis. For validation of the registration procedure the location of the activated regions has been compared with published literature data from electrophysiological recordings or fMRI studies (Spenger et al., 2000; Schweinhardt et al., 2003; Ramu et al., 2006). For this purpose, CMA and CEN of the activation maps have been calculated for each animal. CMA and CEN coordinates for the left and right forepaw of individual animals are displayed in Fig. 2d, with the x-coordinate giving the distance from the midline and the y-coordinate the distance rostral to Bregma (in mm). The corresponding values of the left hemisphere (right forepaw) were mirrored to that of the right hemisphere to allow a comparison of potential left/right asymmetries. The relative CMA and the CEN were found to match almost perfectly for individual animals. Furthermore CMA and CEN values differed only minimally among animals. Numerical values are given in Table 1. The CMA coordinates were in excellent agreement with published values for the forepaw S1 region as derived from electrophysiological recordings and also with values from earlier fMRI studies. The individual data cluster within an area of 1×1 mm^2, revealing the high reproducibility of the activation.

Table 1
Location of forepaw and hindpaw S1 area in intact Lewis rats of 250 g body weight (CMA: center-of-mass, CEN: centroid) for this work

	Forepaw S1		Hindpaw S1		Reference
	x±SE [mm]	y±SE [mm]	x±SE [mm]	y±SE [mm]	
Electrophysiology	3–4.5 digits: 4	−0.5–1.5 digits: 0	2–3 digits: 2.4	0 to −2 digits: −1.8	Chapin and Lin (1984)
fMRI	4.0±0.2	1.0±0.2	2.3±0.1	−1.7±0.1	Endo et al. (2007)
fMRI	3.4±0.4	0.2	2.0±0.6	−0.8	Spenger et al. (2000)
fMRI	3.2±0.4	−1.6±0.2	n.d.	n.d.	Ramu et al. (2006)
fMRI	3.6	−1.8	n.d.	n.d.	Schweinhardt et al. (2003)
CMA right paw	−3.8±0.2	0.4±0.1	−2.4±0.6;	−2.0±0.3	This work
CEN right paw	−3.8±0.2	0.4±0.2	−2.3±0.6	−2.0±0.3	
CMA left paw	+3.7±0.2	0.5±0.2	n.d.	n.d.	
CEN left paw	+3.6±0.3	0.4±0.3	n.d.	n.d.	

Values are indicated as mean±standard error (SE) in [mm] and compared to reference values from literature.
Positive x-values: right hemisphere.
Positive y-values: rostral from Bregma; negative y-values: caudal from Bregma.
n.d. not determined.

Please cite this article as: Sydekum, E. et al., Functional reorganization in rat somatosensory cortex assessed by fMRI: Elastic image registration based on structural landmarks in fMRI images and application to spinal cord injured rats, NeuroImage (2008), doi:10.1016/j.neuroimage.2008.10.015

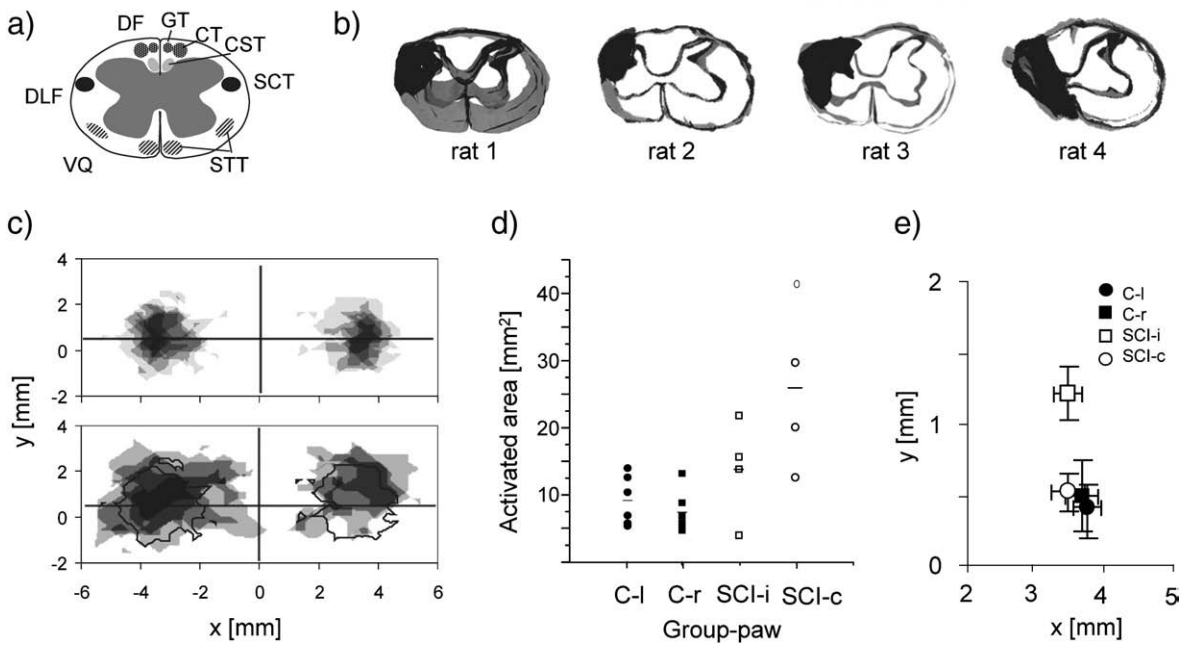

Fig. 3. Effect of unilateral spinal cord injury (SCI) at cervical levels C3/C4 on topology of BOLD-fMRI response: (a) schematic cross-section through spinal cord showing the fiber tracts of concern: gracile tract (GT), cuneate tract (CT), corticospinal tract (CS), spinocervical tract (SCT) and spinothalamic tract (STT). Furthermore dorsal funiculus (DF), dorsolateral funiculus (DLF) and ventral quadrant (VQ) are marked; (b) Reconstruction of lesion site, which partly comprised spinothalamic and spinocervical tracts. In animal 4 the lesion additionally includes ventral tracts. (c) Increase of spatial extent of fMRI response due to SCI, showing activated area in control (upper panel) and SCI rats (lower panel). The right side of the lower panel corresponds to ipsilesional forepaw stimulation and the left side to contralesional paw stimulation respectively. The intensity of the shading represents the number of animals showing a response in the respective area. (d) Quantitative analysis of activation area for individual animals of the control group (left/right paw (C-l; C-r)) and SCI animals (ipsilesional/contralesional (SCI-i; SCI-c)). A significant increase is observed when stimulating the contralesional forepaw, while the effect is less pronounced when stimulating the ipsilesional paw. (e) Center of mass (CMA) for activated S1 area in control and SCI rats. The CMA for the SCI rats is shifted rostrally when stimulating the ipsilesional forepaw.

There was no left–right asymmetry with regard to CMA and CEN values (Table 1).

Blood pressure measurements revealed an increase in mean arterial blood pressure (MABP) starting immediately after stimulation onset and reaching ΔMAPB of 9.4±1.07 (SE) mmHg at the end of the stimulation block. At the end of the stimulation period MABP decreased to reach pre-stimulation values of 77.4±1.5 (SE) mmHg at the end of the stimulation period.

Spinal cord injury induced changes

To clarify the readouts the terms ipsi- and contralesional have been used to indicate the paw stimulated in SCI animals in relation to the injury side, while in all cases the fMRI responses have been observed in the hemisphere contralateral to the paw stimulated. Immediately after an incomplete spinal cord hemisection injury, the ipsilesional forelimb was seldom used; however, this limb was used regularly 2–3 weeks after injury. When skilled locomotion of the ipsilesional forelimb was evaluated 8 weeks after injury, minor deficits were still prevalent to recover completely by 10 weeks. The somatotopic representation of the compensating contralesional forelimb and the recovering ipsilesional forelimb might be distinct from representations in intact animals. We applied the registration procedure to monitor changes in cortical representation of the rat forepaw after injury. Following termination of the fMRI studies the animals were sacrificed and the lesion site was reconstructed histologically. The extent of the injury for individual animals is indicated in Fig. 3 together with a schematic drawing of spinal cord with the fiber tracts of concern (Figs. 3a, b). In rats 1, 2 and 3, the lesion comprised parts of spinothalamic and spinocervical tracts. Animal 4 shows a larger lesion that additionally includes ventral tracts. The somatosensory stimulation was conducted for both forepaws, ipsi and contralateral to the injured side. In both cases, the fMRI response was confined to the corresponding hemisphere.

Despite apparent differences in lesion extent among the animals they displayed similar fMRI responses to the forepaw stimulation. The variability was larger than in uninjured animals. Although the extent of the injury was limited to one side of the spinal cord the cortical BOLD signal was found to be affected in response to stimulation of both injured and uninjured forepaw. The overlay of the activated areas is displayed in Fig. 3c with the line indicating the maximum extent of the activation observed in control animals. Quantitative analysis revealed a significant increase ($p<0.05$) in the corresponding area S1 when stimulating the contralesional paw. The values for the individual animals are displayed in Fig. 3d. Similar, for stimulation of the ipsilesional paw the area of the activated S1 territory tended to increase, but the effect did not reach significance due to the lack of a BOLD response in the most caudal part. In general, functional maps of injured animals show higher variability and often expand over the former functional forepaw borders. The CMA analysis revealed a significant rostral shift for area S1 activated by stimulation of the ipsilesional paw ($p<0.05$), while the CMA corresponding to the contralesional paw was unchanged as compared to the control situation (Fig. 3e). Numerical values are given in Table 2. Analysis of the two imaging sections revealed that all area expansions were restricted to the superficial imaging section.

Table 2
Location of activated forepaw somatosensory area S1 following spinal cord hemisection given as center-of-mass (CMA) and centroid (CEN)

		x±SE [mm]	y±SE [mm]
Ipsilesional paw	CEN	3.48±0.19	1.21±0.19
	CMA	3.47±0.17	1.24±0.20
Contralesional paw	CEN	−3.47±0.23	0.51±0.13
	CMA	−3.46±0.22	0.48±0.12

Values in [mm], (mean±SE).
Positive x-values: right hemisphere (corresponding to stimulation of the ipsilesional paw); negative x-values: left hemisphere (corresponding to stimulation of the contralesional paw).
Positive y-values: rostral from Bregma.

Please cite this article as: Sydekum, E. et al., Functional reorganization in rat somatosensory cortex assessed by fMRI: Elastic image registration based on structural landmarks in fMRI images and application to spinal cord injured rats, NeuroImage (2008), doi:10.1016/j.neuroimage.2008.10.015

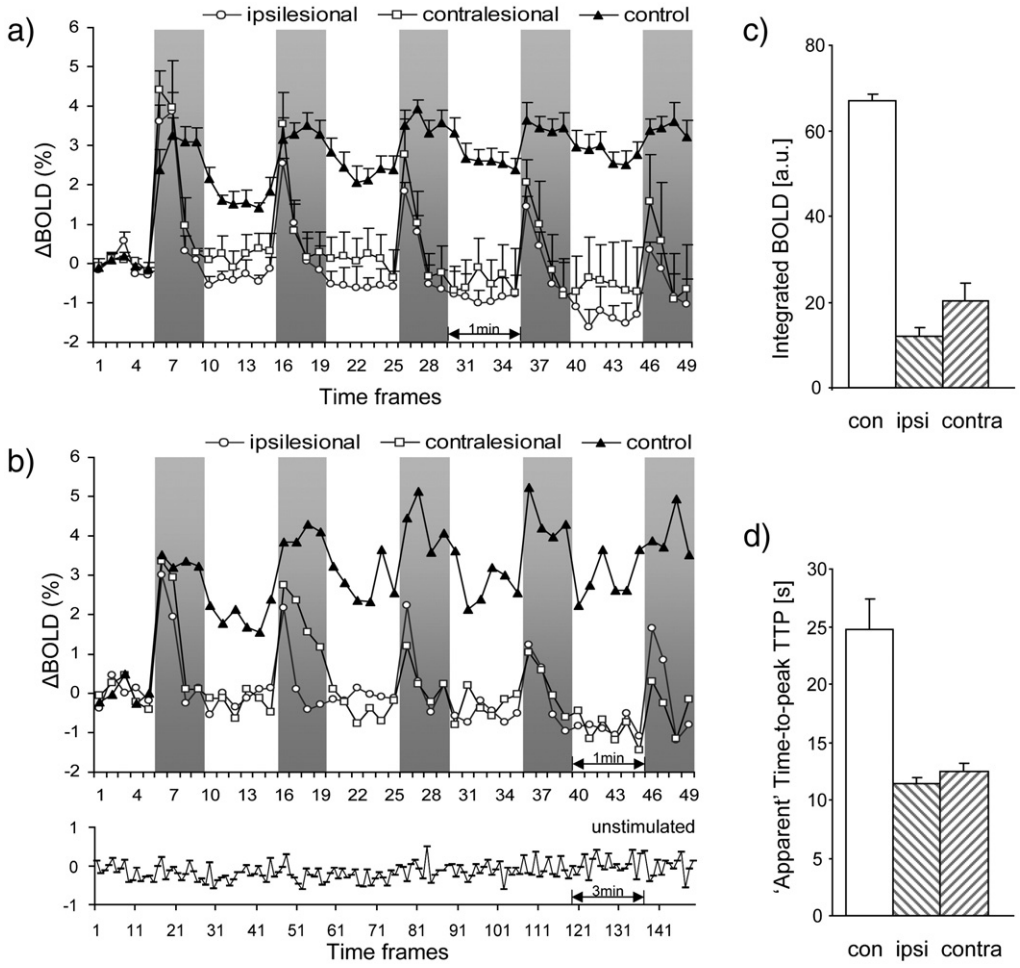

Fig. 4. Effect of SCI on temporal profile of fMRI response for electrical forepaw stimulation (amplitude: 6 mA): (a) BOLD fMRI response as a function of time in control and SCI injured rats. The stimulation periods are indicated by the shaded bars. Temporal resolution is 10 s. Note that the signal in control rats has a 'fast' (correlated with stimulus) and a 'slow' component, triggered by the first onset stimulation and persisting until the end of the 5th stimulation episode. This 'slow' component is not observed in SCI animals. (b) BOLD fMRI response as a function of time for an individual control and a SCI animal to illustrate signal to noise ratio (SNR). Signal represents average intensity over all voxels in the ROI within the somatosensory S1 area showing activation. On the lower axis a trace reflecting signal fluctuations in S1 without stimulation is shown for an extended measurement period lasting 25 min. (c) The integrated BOLD response is reduced in SCI rats primarily due to the absence of the slow component. (d) The 'apparent' time-to-peak (TPP) is significantly reduced in SCI rats both for the stimulation of the ipsilesional (ipsi) and the contralesional (contra) forepaw.

More striking than the changes in the spatial extent of the activated S1 region as a result of SCI were the changes in the temporal profile to the sensory S1 response. Fig. 4a depicts the mean signal amplitude in the activated area as a function of time for the five stimulation episodes. Interestingly the responses to both ipsi- and contralesional forepaw stimulation were almost identical, but differed significantly from the control pattern. For control animals the responses of the two sides have been found identical within error limits and were therefore pooled. Two parameters have been extracted from the curve: the integral under the BOLD curve and the average time after stimulation onset until the maximal response was reached. The integral value was significantly decreased for SCI rats with no difference between ipsi- and contralesional forepaw stimulation (Fig. 4c, $p<0.05$). This is due to the fact that 1) in lesioned rats the BOLD response is characterized through a fast burst response and a rapid drop in signal intensity despite ongoing stimulation. Control animals in contrast show maximal signal amplitude in the second half of each stimulation phase at around 25 s ($p<0.05$, Fig. 4d). 2) There is an underlying slow component observed in control animals that did not recover during the 60 s in-between subsequent stimulation blocks. Quantitative data for the temporal profile of the BOLD signal are just shown for the superficial section. The lower section revealed the same dynamics, but suffered from higher level of noise probably as a consequence of the surface coil used. Furthermore the signal amplitude was reduced in the lower section what is in line with the results shown in previous studies (Silva and Koretsky, 2002). Table 3 shows behavioral data from the horizontal ladder paradigm for two time points before fMRI was performed. The ipsilesional forepaw shows improvement over time from slight impairment to almost full performance, whereby the contralesional forepaw has not been affected at any time point.

For assessment of data quality "raw data" traces for an individual control and an SCI animal showing signal time curves of the activated area are presented in Fig. 4b. Fluctuations in baseline blood flow have been observed under isoflurane anaesthesia (Kannurpatti et al., 2008).

Table 3
Performance of rat 1 to 4 in horizontal ladder test following spinal cord injury at 8 and 10 weeks (fMRI at 12 weeks)

Rat	Forelimb			
	Ipsilesional		Contralesional	
	8 weeks	10 weeks	8 weeks	10 weeks
1	73	89	100	100
2	70	100	100	100
3	100	100	100	100
4	80	98	100	100

Values are given in % successful steps, defined as number of correct steps out of total number of steps for both forepaws (ipsilesional and contralesional).

Please cite this article as: Sydekum, E. et al., Functional reorganization in rat somatosensory cortex assessed by fMRI: Elastic image registration based on structural landmarks in fMRI images and application to spinal cord injured rats, NeuroImage (2008), doi:10.1016/j.neuroimage.2008.10.015

Therefore an extended baseline trace (lower axis in Fig. 4b) reflecting S1 signal dynamics has been recorded without stimulation demonstrating the hemodynamic stability achieved using our experimental protocol with controlled ventilation of the animals under isoflurane anaesthesia.

Discussion

Changes in the (macroscopic) functional topology in response to physiological or pathological stimuli such as focal lesions of the central nervous system are, in general, slow processes occurring over weeks or months. Monitoring functional reorganization both in individuals and by group comparisons e.g. using fMRI techniques, therefore, requires tools for accurate co-registration of imaging data sets acquired in different imaging sessions (or different individuals). In order to map temporo-spatial changes in the functional response the imaging modality should provide i) large volume coverage of the region of interest and ii) high temporal resolution. In the current study, we monitored the changes elicited by partial SCI in the rat somatosensory cortical fMRI response caused by sensory forepaw stimulation. Correspondingly, the imaging technique should yield sufficient coverage of the cortical S1 region and a temporal resolution of the order of a few seconds.

Recording few slices in horizontal orientation allows covering a large fraction of the rat cerebral cortex with adequate spatial and temporal resolution. Two adjacent horizontal slices were sufficient to cover the cortical region of interest and allowed analysis of the temporal response of the fMRI signal after injury (see below). In contrast, the more conventional coronal slice orientation yields lower resolution within the horizontal plane, i.e. parallel to the cortical surface, as one pixel dimension is determined by the slice thickness. On the other hand, due to the higher resolution within the coronal plane it allows resolving cortical layers (Silva and Koretsky, 2002). In addition, covering large cortical areas would require a significantly higher number of slices and would correspondingly deteriorate time resolution. Similarly, full three-dimensional data acquisition would be time consuming.

A critical aspect, when studying the cortical functional topology involving groups of animals, is the proper registration of the EPI-based fMRI images, which are prone to geometrical distortions due to artifacts caused by alterations in magnetic susceptibility at tissue interfaces. Therefore, it is essential to define landmarks for image registration on the fMRI images themselves. In the current study, we have used three landmarks that could be determined in a highly reproducible manner in EPI images: i) the Bregma, i.e. the intersection of the coronal suture with the brain midline, ii) the most rostral point of the cerebellum, and iii) the maximal width of the right hemisphere in the ventral imaging slice. Using the three landmarks and correcting the images with the linear scaling factors derived, adequate registration to the coordinates of the reference atlas could be achieved. A limitation of this approach is that it does not account for irregular distortions, which cannot be corrected using linear scaling. More complex image transformation requires significantly more landmark points (Ashburner and Friston, 1999). Yet, cortical EPI images using short echo times intrinsically display little contrast and thus little structure. Increasing echo times would enhance contrast at the expense of larger distortions and signal losses due to changes in magnetic susceptibility at tissue interfaces. Similarly the use of alternative MRI sequences that provide better anatomical definition is not feasible as susceptibility based distortions are sequence specific. Therefore, the definition of unique reference points from EPI images is challenging. As shown in this study, major cortical vessels might constitute valuable landmarks.

The Bregma point was deduced from the blood vessel induced signal voids in the EPI scans. In standard small animal fMRI procedures vascular landmarks are not routinely used; however, the vascularization pattern is widely used as a reliable landmark in electrophysiological studies of rat barrel cortex (Woolsey et al., 1996). Obviously the quality of a landmark depends on its geometrical reproducibility. Evaluation of the degree of variability in the position of the veins underlying the coronal suture in four rats revealed that the vascular anatomy for these veins is highly conserved. The intersection with the midline corresponds with the Bregma, which is confirmed by the fact that the distance between this point and the rostral end of the cerebellum corresponds to the value derived from the rat brain atlas.

The good agreement between the activated S1 areas obtained using the registered image data from this study (CMA and CEN) with published values from electrophysiological and optical imaging studies that have been reported in relation to stereotactic coordinates reveals that the elastic registration with bilinear scaling yields accurate information. Further empirical proof for the appropriateness of the scaling factors s_x and s_y is the precise localization of the hindpaw area relative to forepaw with the border zone well defined and without spatial overlap in agreement with previous electrophysiological studies.

The primary somatosensory cortex (S1) is organized into well distinct representations. Alterations in incoming signal patterns, e.g. in response to a spinal cord injury, may induce reorganization of these cortical representations. Having demonstrated a high degree of reproducibility of functional representations among intact animals, the fMRI approach was used to investigate map changes associated with sensory input altered by an injury. We detected a significant increase in BOLD-fMRI representation in cortical S1 when stimulating the contralesional forepaw. Immediately after injury the young animals (28 days) were unable to adequately use the ipsilesional limb, they consequently had to relay more on the intact, contralesional limb. This may have induced altered cortical excitability (Hains et al., 2003) and an expanded forepaw sensory representation of the S1 cortex corresponding to the intact limb. Similar expansion of BOLD-fMRI forepaw representations has also been documented in large thoracic spinal cord injuries that causes paralysis of hindlimbs (Endo et al., 2007). After these large lesions, forelimbs may have compensated for the lacking hindlimb functions.

The activation map corresponding to the ipsilesional forepaw, which revealed behavioral deficits at an early time point, shifted rostrally (center of mass and centroid). The observed dislocation is caused by both, an expansion of the former forepaw boarder zone rostrally and also by an activation loss in caudal direction. The latter phenomenon might be caused by the fact that the lesion was in close proximity to the lateral regions of the dorsal funiculus, which comprise sensory tracts that carry information from the spinal segments relevant to the forepaw (Pfaller and Arvidsson, 1988; Arvidsson and Pfaller, 1990). Both observations taken together indicate a significant shift of cortical functional representations. All area expansions seen in the injured animals were restricted to the superficial imaging plane, which includes the metabolically most active input layer IV but also contributions from large pial veins. However, it should be kept in mind that a shift in the functional border does not necessarily imply a shift in the anatomical border (Hickmott and Steen, 2005) as reorganization might occur by modification of synaptic strength in pre-existing circuits (Raineteau and Schwab, 2001). Unmasking of preexisting connections could occur as a result of the injury, which might influence inhibitory circuits. Mechanisms therefore could be i.e. increased excitatory neurotransmitter release, enhanced postsynaptic effects of weak inputs by changes in membrane conductance or, as a result of disturbed inhibitory projections, reduced inhibitory interactions. (Navarro et al., 2007); all those factors are potentially of relevance in the animal's compensatory strategies. The fact that SCI affects both fibers that cross the midline as well as fibers that do not (Kobayashi, 1998) might explain the observation that the fMRI response is compromised on both sides.

Please cite this article as: Sydekum, E. et al., Functional reorganization in rat somatosensory cortex assessed by fMRI: Elastic image registration based on structural landmarks in fMRI images and application to spinal cord injured rats, NeuroImage (2008), doi:10.1016/j.neuroimage.2008.10.015

Irrespective of the paw stimulated, (ipsilesional and contralesional), changes in BOLD profiles in the S1 sensory cortex have been observed in all injured rats, which displayed both a significantly reduced "apparent" time to peak (TTP) after stimulation onset for all stimulation episodes and reduced integrated BOLD amplitude. The most striking effect observed in SCI rats, however, is the fast signal decay of the BOLD response even during ongoing stimulation after a fast burst response which is in line with the reduced "apparent" time to peak, the lack of the underlying slow signal component and, as a consequence, reduced overall BOLD signal change.

We have to consider that the BOLD response could be influenced by the specific stimulation protocol used. Isoflurane anaesthesia, which is established for small animal fMRI (Sauter et al., 2002; Liu et al., 2004; Masamoto et al., 2007) has been chosen because isoflurane has the stability of anaesthetic depth coupled with the ease of simple noninvasive induction and is appropriate for long term studies. Isoflurane has been known to cause vasodilatation of cerebral arteries and intraparenchymal arterioles which may affect the vascular reactivity to local neural activation (Masamoto et al., 2007). Higher baseline CBF has been observed for animals under isoflurane anaesthesia: different baseline CBF would significantly affect the magnitude of stimulation-induced hemodynamic responses (Detsch et al., 1999). Yet we have been careful to maintain physiological conditions in the rats as comparable as possible (respiratory frequency, tidal volumes, temperature, pCO_2) to minimize this variability and avoid a baseline drift over the measurement period as shown for the non-stimulated state (see Fig. 4b, lower axis). Moreover, the reproducibility of data both with regard to the spatial extent and the temporal response demonstrates the suitability of this anaesthesia protocol for studies of functional plasticity. However, in every case the stimulation condition has to be adapted to the specific anaesthesia protocol: e.g. stimulation parameters optimized for α-chloralose may not be adequate when using isoflurane anaesthesia and vice versa.

As the injury affected mainly spino thalamic tracts (STT) a rather high stimulation amplitude of 6 mA was chosen, which causes not only excitation of cutaneous and subcutaneous mechanoreceptors transmitting sensory information but also nociceptors, which are activated at higher stimulation thresholds (Endo et al., 2008). STT, which have their cell bodies in the spinal cord dorsal horn, relay nociception to the contralateral somatosensory cortex somatotopically through axons projecting across the midline (Schouenborg et al., 1986). The STT receives its inputs from the unmyelinated C-fibers and from myelinated Aδ fibers. While Aδ fibers can transmit nociception, thermosensation and touch, C-fibers transmit nociception and thermosensation but not touch (Leem et al., 1993). Nociceptive signals, which are propagated through different tracts than sensory signals, also show different temporal response profiles (Chang and Shyu, 2001).

Slow signal components have been shown before in CBV measurements using long stimulation paradigms (Silva et al., 2007). However, in contrast to our study the prolonged return to baseline was not present for the BOLD contrast. A potential explanation for the slow signal component observed for the control animals in our study is persistence of baseline blood flow increase beyond the stimulation period. Veins are surrounded by smooth muscle, which is a viscoelastic material exhibiting stress relaxation. Therefore a step increase in pressure produces a rapid elastic expansion followed by a slow further increase in volume over a period of minutes as explained in the windkessel model (Mandeville et al., 1999). This would be in line with the blood pressure increase observed after stimulation onset. The change in MABP was modest and normally a decrease in cerebrovascular resistance would compensate for this thereby maintaining flow relatively constant (Tuor et al., 2002).

The absence of this drift in the fMRI signal profile of SCI animals might be due to the fact that the SCI (partly) affected both slow pain and sensory fibers. Therefore sensory and nociceptive inputs are altered, which might result in the burst response observed. Alternatively, in SCI rats the excitatory input due to electrical forepaw stimulation might be dominated by an inhibitory input following the fast initial response or that an excitatory, facilitating influence is missing after injury while the inhibitory is still intact (Li and Zhuo, 2001; Gebhart, 2004).

At this stage interpretations remain speculative and further studies using differential stimulation paradigms and/or pharmacological interventions are required to fully understand the various components of the fMRI signal in the rat somatosensory cortex and how they are influenced by partial SCI.

Conclusions

fMRI allows studying the functional topography and plasticity of the rodent brain. Due to its non-invasiveness plastic processes can be monitored over extended periods of time in individual animals. As the rodent cortex lacks gyration and is organized as quasi two-dimensional functional map, two-dimensional fMRI using a horizontal slice orientation is optimally suited for studying the cortical organization. The method provides coverage of large cortical areas, adequate in-plane spatial resolution and also adequate temporal resolution to study the fMRI response in a dynamic fashion. A critical aspect for such studies is proper registration of fMRI images, which due to the EPI sequences used are inherently distorted as a consequence of differences in local magnetic susceptibility. Compensation for these effects requires elastic registration procedures using landmarks identified on the EPI based fMRI images. Conventional rigid body transformation does not yield the accuracy required; instead, bilinear elastic scaling allowed mapping of fMRI images using co-registered anatomical landmarks of the rat brain and has turned out essential for detecting minor changes in the functional topology. The accuracy of the procedure has been verified by analyzing the response in the somatosensory S1 area following fore and hindpaw stimulation. In a rat spinal cord lesion model the registration procedure allowed detecting changes in extent and location of forepaw S1 area induced by small unilateral tract lesions. In addition, the temporal response was found to be severely affected by the lesion. The signal profiles indicated the involvement of multiple spinal tracts in signal processing.

Acknowledgments

The authors thank the NCCR Neural Plasticity and Repair and the Swiss National Science Foundation for funding this project.

References

Arvidsson, J., Pfaller, K., 1990. Central projections of C4–C8 dorsal root ganglia in the rat studied by anterograde transport of WGA-HRP. J. Comp. Neurol. 292, 349–362.
Ashburner, J., Friston, K.J., 1999. Nonlinear spatial normalization using basis functions. Hum. Brain Mapp. 7, 254–266.
Benderbous, S., Corot, C., Jacobs, P., Bonnemain, B., 1996. Superparamagnetic agents: physicochemical characteristics and preclinical imaging evaluation. Acad. Radiol. 3 (Suppl. 2), S292–S294.
Bock, C., Krep, H., Brinker, G., Hoehn-Berlage, M., 1998. Brainmapping of alpha-chloralose anesthetized rats with T2*-weighted imaging: distinction between the representation of the forepaw and hindpaw in the somatosensory cortex. NMR Biomed. 11, 115–119.
Chang, C., Shyu, B.C., 2001. A fMRI study of brain activations during non-noxious and noxious electrical stimulation of the sciatic nerve of rats. Brain Res. 897, 71–81.
Chapin, J.K., Lin, C.S., 1984. Mapping the body representation in the SI cortex of anesthetized and awake rats. J. Comp. Neurol. 229, 199–213.
Chen, Z., Shen, J., 2006. Single-shot echo-planar functional magnetic resonance imaging of representations of the fore- and hindpaws in the somatosensory cortex of rats using an 11.7 T microimager. J. Neurosci. Methods 151, 268–275.
Coq, J.O., Xerri, C., 1999. Tactile impoverishment and sensorimotor restriction deteriorate the forepaw cutaneous map in the primary somatosensory cortex of adult rats. Exp. Brain Res. 129, 518–531.
Detsch, O., Vahle-Hinz, C., Kochs, E., Siemers, M., Bromm, B., 1999. Isoflurane induces dose-dependent changes of thalamic somatosensory information transfer. Brain Res. 829, 77–89.

Please cite this article as: Sydekum, E. et al., Functional reorganization in rat somatosensory cortex assessed by fMRI: Elastic image registration based on structural landmarks in fMRI images and application to spinal cord injured rats, NeuroImage (2008), doi:10.1016/j.neuroimage.2008.10.015

Duong, T.Q., Silva, A.C., Lee, S.P., Kim, S.G., 2000. Functional MRI of calcium-dependent synaptic activity: cross correlation with CBF and BOLD measurements. Magn. Reson. Med. 43, 383–392.
Endo, T., Spenger, C., Tominaga, T., Brene, S., Olson, L., 2007. Cortical sensory map rearrangement after spinal cord injury: fMRI responses linked to Nogo signalling. Brain 130, 2951–2961.
Endo, T., Spenger, C., Hao, J., Tominaga, T., Wiesenfeld-Hallin, Z., Olson, L., Xu, X.J., 2008. Functional MRI of the brain detects neuropathic pain in experimental spinal cord injury. Pain 138, 292–300.
Frahm, J., Haase, A., Matthaei, D., 1986. Rapid NMR imaging of dynamic processes using the FLASH technique. Magn. Reson. Med. 3, 321–327.
Gebhart, G.F., 2004. Descending modulation of pain. Neurosci. Biobehav. Rev. 27, 729–737.
Grieve, S.M., Blamire, A.M., Styles, P., 2000. The effect of bulk susceptibility on murine snapshot imaging at 7.0 T: a comparison of snapshot imaging techniques. Magn. Reson. Med. 43, 747–755.
Gruetter, R., 1993. Automatic, localized in vivo adjustment of all first- and second-order shim coils. Magn. Reson. Med. 29, 804–811.
Grune, M., Pillekamp, F., Schwindt, W., Hoehn, M., 1999. Gradient echo time dependence and quantitative parameter maps for somatosensory activation in rats at 7 T. Magn. Reson. Med. 42, 118–126.
Hains, B.C., Willis, W.D., Hulsebosch, C.E., 2003. Serotonin receptors 5-HT1A and 5-HT3 reduce hyperexcitability of dorsal horn neurons after chronic spinal cord hemisection injury in rat. Exp. Brain Res. 149, 174–186.
Henning, J., Nauerth, A., Friedburg, H., 1986. RARE imaging: a fast imaging method for clinical MR. Magn. Reson. Med. 3, 823–833.
Hickmott, P.W., Steen, P.A., 2005. Large-scale changes in dendritic structure during reorganization of adult somatosensory cortex. Nat. Neurosci. 8, 140–142.
Hyder, F., Behar, K.L., Martin, M.A., Blamire, A.M., Shulman, R.G., 1994. Dynamic magnetic resonance imaging of the rat brain during forepaw stimulation. J. Cereb. Blood Flow Metab. 14, 649–655.
Jezzard, P., Clare, S., 1999. Sources of distortion in functional MRI data. Hum. Brain Mapp. 8, 80–85.
Kannurpatti, S.S., Biswal, B.B., Kim, Y.R., Rosen, B.R., 2008. Spatio-temporal characteristics of low-frequency BOLD signal fluctuations in isoflurane-anesthetized rat brain. NeuroImage 40, 1738–1747.
Keilholz, S.D., Silva, A.C., Raman, M., Merkle, H., Koretsky, A.P., 2004. Functional MRI of the rodent somatosensory pathway using multislice echo planar imaging. Magn. Reson. Med. 52, 89–99.
Kennerley, A.J., Berwick, J., Martindale, J., Johnston, D., Papadakis, N., Mayhew, J.E., 2005. Concurrent fMRI and optical measures for the investigation of the hemodynamic response function. Magn. Reson. Med. 54, 354–365.
Kobayashi, Y., 1998. Distribution and morphology of spinothalamic tract neurons in the rat. Anat. Embryol. (Berl) 197, 51–67.
Leem, J.W., Willis, W.D., Chung, J.M., 1993. Cutaneous sensory receptors in the rat foot. J. Neurophysiol. 69, 1684–1699.
Li, P., Zhuo, M., 2001. Cholinergic, noradrenergic, and serotonergic inhibition of fast synaptic transmission in spinal lumbar dorsal horn of rat. Brain Res. Bull. 54, 639–647.
Liu, Z.M., Schmidt, K.F., Sicard, K.M., Duong, T.Q., 2004. Imaging oxygen consumption in forepaw somatosensory stimulation in rats under isoflurane anaesthesia. Magn. Reson. Med. 52, 277–285.
Logothetis, N.K., 2008. What we can do and what we cannot do with fMRI. Nature 453, 869–878.
Mandeville, J.B., Marota, J.J., Ayata, C., Zaharchuk, G., Moskowitz, M.A., Rosen, B.R., Weisskoff, R.M., 1999. Evidence of a cerebrovascular postarteriole windkessel with delayed compliance. J. Cereb. Blood Flow Metab. 19, 679–689.
Mansfield, P., 1984. Real-time echo-planar imaging by NMR. Br. Med. Bull. 40, 187–190.
Marota, J.J., Ayata, C., Moskowitz, M.A., Weisskoff, R.M., Rosen, B.R., Mandeville, J.B., 1999. Investigation of the early response to rat forepaw stimulation. Magn. Reson. Med. 41, 247–252.
Masamoto, K., Kim, T., Fukuda, M., Wang, P., Kim, S.G., 2007. Relationship between neural, vascular, and BOLD signals in isoflurane-anesthetized rat somatosensory cortex. Cereb. Cortex 17, 942–950.
McEwen, M.L., Springer, J.E., 2006. Quantification of locomotor recovery following spinal cord contusion in adult rats. J. Neurotrauma 23, 1632–1653.
Metz, G.A., Merkler, D., Dietz, V., Schwab, M.E., Fouad, K., 2000. Efficient testing of motor function in spinal cord injured rats. Brain Res. 883, 165–177.
Navarro, X., Vivo, M., Valero-Cabre, A., 2007. Neural plasticity after peripheral nerve injury and regeneration. Prog. Neurobiol. 82, 163–201.
Neafsey, J.E., 1990. The complete ratunculus: output organization of layer V of the cerebral cortex. In: Kolb, B., Tees, R.C. (Eds.), The Cerebral Cortex of the Rat. MIT Press, Cambridge.
Paxinos, G., Watson, C., 1998. The Rat Brain in Stereotactic Coordinates. Academic Press.
Paxinos, G., Watson, C., Pennisi, M., Topple, A., 1985. Bregma, lambda and the interaural midpoint in stereotaxic surgery with rats of different sex, strain and weight. J. Neurosci. Methods 13, 139–143.
Pfaller, K., Arvidsson, J., 1988. Central distribution of trigeminal and upper cervical primary afferents in the rat studied by anterograde transport of horseradish peroxidase conjugated to wheat germ agglutinin. J. Comp. Neurol. 268, 91–108.
Raineteau, O., Schwab, M.E., 2001. Plasticity of motor systems after incomplete spinal cord injury. Nat. Rev. Neurosci. 2, 263–273.
Ramu, J., Bockhorst, K.H., Mogatadakala, K.V., Narayana, P.A., 2006. Functional magnetic resonance imaging in rodents: methodology and application to spinal cord injury. J. Neurosci. Res. 84, 1235–1244.
Sauter, A., Reese, T., Porszasz, R., Baumann, D., Rausch, M., Rudin, M., 2002. Recovery of function in cytoprotected cerebral cortex in rat stroke model assessed by functional MRI. Magn. Reson. Med. 47, 759–765.
Schouenborg, J., Kalliomaki, J., Gustavsson, P., Rosen, I., 1986. Field potentials evoked in rat primary somatosensory cortex (SI) by impulses in cutaneous A beta- and C-fibres. Brain Res. 397, 86–92.
Schweinhardt, P., Fransson, P., Olson, L., Spenger, C., Andersson, J.L., 2003. A template for spatial normalisation of MR images of the rat brain. J. Neurosci. Methods 129, 105–113.
Sheth, S., Nemoto, M., Guiou, M., Walker, M., Pouratian, N., Toga, A.W., 2003. Evaluation of coupling between optical intrinsic signals and neuronal activity in rat somatosensory cortex. NeuroImage 19, 884–894.
Sheth, S.A., Nemoto, M., Guiou, M., Walker, M., Pouratian, N., Hageman, N., Toga, A.W., 2004. Columnar specificity of microvascular oxygenation and volume responses: implications for functional brain mapping. J. Neurosci. 24, 634–641.
Silva, A.C., Koretsky, A.P., 2002. Laminar specificity of functional MRI onset times during somatosensory stimulation in rat. Proc. Natl. Acad. Sci. U. S. A. 99, 15182–15187.
Silva, A.C., Koretsky, A.P., Duyn, J.H., 2007. Functional MRI impulse response for BOLD and CBV contrast in rat somatosensory cortex. Magn. Reson. Med. 57, 1110–1118.
Spenger, C., Josephson, A., Klason, T., Hoehn, M., Schwindt, W., Ingvar, M., Olson, L., 2000. Functional MRI at 4.7 tesla of the rat brain during electric stimulation of forepaw, hindpaw, or tail in single- and multislice experiments. Exp. Neurol. 166, 246–253.
Stefanovic, B., Schwindt, W., Hoehn, M., Silva, A.C., 2007. Functional uncoupling of hemodynamic from neuronal response by inhibition of neuronal nitric oxide synthase. J. Cereb. Blood Flow Metab. 27, 741–754.
Tuor, U.I., McKenzie, E., Tomanek, B., 2002. Functional magnetic resonance imaging of tonic pain and vasopressor effects in rats. Magn. Reson. Imaging 20, 707–712.
Van Camp, N., Verhoye, M., Van der Linden, A., 2006. Stimulation of the rat somatosensory cortex at different frequencies and pulse widths. NMR Biomed. 19, 10–17.
Weber, R., Ramos-Cabrer, P., Wiedermann, D., van Camp, N., Hoehn, M., 2006. A fully noninvasive and robust experimental protocol for longitudinal fMRI studies in the rat. NeuroImage 29, 1303–1310.
Woolsey, T.A., Rovainen, C.M., Cox, S.B., Henegar, M.H., Liang, G.E., Liu, D., Moskalenko, Y.E., Sui, J., Wei, L., 1996. Neuronal units linked to microvascular modules in cerebral cortex: response elements for imaging the brain. Cereb. Cortex 6, 647–660.
Xerri, C., Bourgeon, S., Coq, J.O., 2005. Perceptual context-dependent remodeling of the forepaw map in the SI cortex of rats trained on tactile discrimination. Behav. Brain Res. 162, 207–221.
Xiao, J., 2007. A new coordinate system for rodent brain and variability in the brain weights and dimensions of different ages in the naked mole-rat. J. Neurosci. Methods 162, 162–170.
Yang, X., Hyder, F., Shulman, R.G., 1997. Functional MRI BOLD signal coincides with electrical activity in the rat whisker barrels. Magn. Reson. Med. 38, 874–877.
Zhao, Y., Anderson, A.W., Gore, J.C., 2005. Computer simulation studies of the effects of dynamic shimming on susceptibility artifacts in EPI at high field. J. Magn. Reson. 173, 10–22.

Please cite this article as: Sydekum, E. et al., Functional reorganization in rat somatosensory cortex assessed by fMRI: Elastic image registration based on structural landmarks in fMRI images and application to spinal cord injured rats, NeuroImage (2008), doi:10.1016/j.neuroimage.2008.10.015